

A CMOS Bio-Impedance Measurement System

Alberto Yúfera and Adoración Rueda

Instituto de Microelectrónica de Sevilla (IMSE), Centro Nacional de Microelectrónica (CNM-CSIC)
Universidad de Sevilla

Av. Américo Vespucio s/n. 41092. Sevilla. SPAIN

Email: {yufera,rueda}@imse.cnm.es

Abstract -- This paper proposes a new method for bio-impedance measurement useful to 2D processing of cell cultures. It allows to represent biological samples by using a new impedance sensing method, and exploiting the electrode-to-cell model for both electrical simulation and imaging reconstruction. Preliminary electrical simulations are reported to validate the proposal for Electrical Cell Impedance Spectroscopy (ECIS) applications. The results reported show that low concentration cell culture can be correctly sensed and displayed at several frequencies using the proposed CMOS system.

keywords -- Bioimpedance, biometric circuits, CMOS analog circuits, bio-instrumentation, sensory systems.

I. INTRODUCTION

The impedance is an useful parameter for determining the properties of biological materials because these are conductives [1] and impedance measurement represents a non-invasive technique. Many biological parameters and processes can be sensed and monitored using its impedance as marker [2-5]. Impedance Spectroscopy of cell culture [6] and Electrical Impedance Tomography (EIT) in bodies [7] are two examples of the impedance utility for measuring biological and medical processes and parameters.

Classical imaging systems for biological samples are based on optical stimulation of samples demanding bulky and expensive equipments. Embedded CMOS sensor have been reported as an alternative to increase the sensitivity to cell location and manipulation. The most popular are optical [10], capacitive [8] and impedance [9] based sensors. In spite of the high number of works with optical sensor in last years, they still need external lamps, optical fibers, etc, while capacitive and impedance based detection do not rely on external equipment.

This paper proposes a new method for impedance measure with applications to cell culture imaging system. The system employs a two dimension electrode array acting as sensor [11,12] together with CMOS circuits for impedance measure [13]. It allows the selection of input frequency to optimize the

sensitivity of electrode sensors and to control, by design, the voltage applied to electrodes for their adequate polarization. The proposed system shown in Fig. 1 includes circuits for exciting and measuring the impedance of each electrode, for addressing rows and columns in the array, and can be fully-integrated in CMOS technologies. When low concentration cell cultures are carried out on top of an electrode array, depending on the position of each cell, a different electrode-cell impedance will be measured, allowing cell detection. Electrical models have been reported for the electrode-cell interfaces [12,14], being these key for matching electrical simulations to real systems performance and hence decoding correctly the results obtained experimentally, usually known as reconstruction problem.

This paper is organized as follows: in section II is described the area parametrized cell-electrode electrical model for both simulation and imaging reconstruction. Proposed CMOS system and circuits for impedance measure are reported in section III. Design system considerations and simulation results for an 8x8 electrode array are given in section IV. Conclusion are underlined in section V.

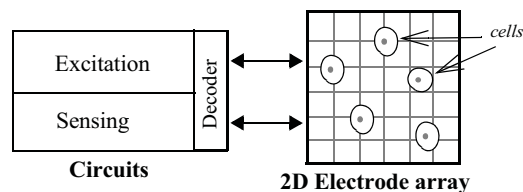


Fig.1. Proposed system for the 2D cell imaging system based on impedance sensing: circuits and two dimension electrode array with cell culture on top.

II. THE CELL-ELECTRODE MODEL

An equivalent circuit for modelling the electrode-cell interface performance is a requisite for electrical characterization of the cells on top of electrodes. Fig. 2 illustrates a two-electrode sensor useful for ECIS technique [12]: e_1 is called sensing electrode and e_2 reference electrode. Electrodes can be fabricated in CMOS process in metal layers [11] or adding post-processing steps [12]. The sample on e_1 top is a cell

This work is in part supported by the Spanish founded Project: TEC2007-68072/TECATE, Técnicas para mejorar la calidad del test y las prestaciones del diseño en tecnologías CMOS submicrométricas.

whose location must be detected. The circuit models developed to characterize electrode-cell interfaces [12,14] contain technology processes information and assume, as main parameter, the overlapping area between cells and electrodes. An adequate interpretation of these models gives information for: a) *electrical simulations*: parametrized models can be used to update the actual electrode circuit in terms of its overlapping with cells. b) *imaging reconstruction*: electrical signals measured on the sensor can be associated to a given overlapping area, obtaining the actual area covered on the electrode from measurements done.

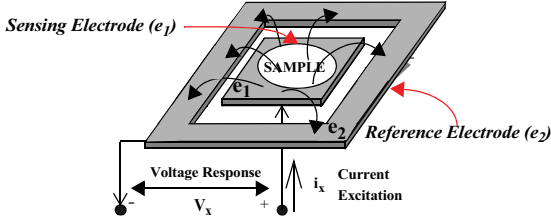


Fig.2. Basic concept for measuring in ECIS technique using two electrodes: e_1 or sensing electrode and e_2 or reference electrode. AC current i_x is injected between e_1 and e_2 , and voltage response V_x is measure from e_1 to e_2 , including effect of e_1 , e_2 and sample impedances.

In this work, we selected the electrode-cell model reported in [12]. This model was obtained by using finite element method simulations, and considers the sensing surface of e_1 could be total or partially filled by cells. Figure 3 shows this model. For the two-electrode sensor in Fig. 2, with e_1 sensing area A , $Z(\omega)$ is the impedance by unit area of the empty electrode (without cells on top). When e_1 is partially covered by cells in a surface A_c , $Z(\omega)/(A-A_c)$ is the electrode impedance associated to non-covered area by cells, and $Z(\omega)/A_c$ is the impedance of the covered area. R_{gap} models the current flowing laterally in the electrode-cell interface, which depends on the electrode-cell distance at the interface (in the range of 10-100nm). R_s is the spreading resistance through the conductive solution. In this model, the signal path from e_1 to e_2 is divided into two parallel branches: one direct branch through the solution, not covered by cells, and a second path containing the electrode area covered by the cells. For the empty electrode, the impedance model $Z(\omega)$ has been chosen as the circuit illustrated in Fig. 3c, where C_p , R_p and R_s are dependent on both electrode and solution materials. Other cell-electrode models can be used [14], but for they the measure method here in proposed is still valid. We have considered for e_2 the model in Fig 3a, not covered by cells. Usually reference electrode is common for all sensors, being its area much higher than e_1 . Figure 4 represents the impedance magnitude, Z_{xoc} , for the sensor system in Fig. 2, considering that e_1 could be either empty, partially or totally covered by cells. The parameter ff is called *fill factor*, being zero for $A_c=0$ (electrode empty), and 1

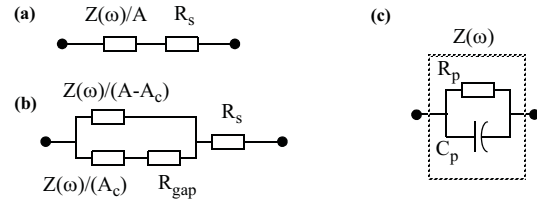


Fig.3. Model for (a) e_1 electrode without cells and (b) e_1 cell-electrode. (c) Model for $Z(\omega)$ used in this work.

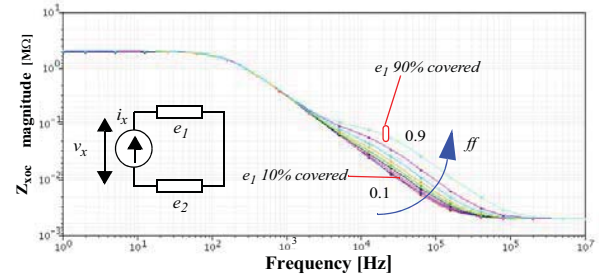


Fig.4. Sensor impedance magnitude as fill factor parameter (ff). $C_p=1nF$, $R_p=1M\Omega$, $R_s=1k\Omega$ and $R_{gap}=100k\Omega$.

for $A_c=A$ (electrode full). We define $Z_{xoc}(ff=0)=Z_{x0}$ as the impedance magnitude of the sensor without cells.

Absolute changes on impedance magnitude of e_1 in series with e_2 are detected in a [10kHz,100kHz] frequency range as a results of sensitivity to area covered on e_1 . Relative changes can inform more accurate from these variations by defining a new figure-of-merit called r [12], or *normalized impedance magnitude*, by the equation,

$$r = \frac{Z_{xoc} - Z_{x0}}{Z_{x0}} \quad (1)$$

where r represents changes of impedance magnitude for the two-electrode with cells (Z_{xoc}) respect to others without them (Z_{x0}). The graphics of r versus frequency is plotted in Fig. 5, for a cell-to-electrode coverage ff from 0.1 to 0.9 in steps of 0.1. It can be identified again the frequency range where the sensitivity to cells is high, represented by r increments. For a given frequency, it can be linked each value of the normalized impedance r with its ff , being possible the cell detection and estimation of the covered area A_c . For imaging reconstruction, this work proposes a new CMOS system to measure r parameter for a given frequency, and to detect the corresponding covering area on each electrode according to sensitivity in Fig 5.

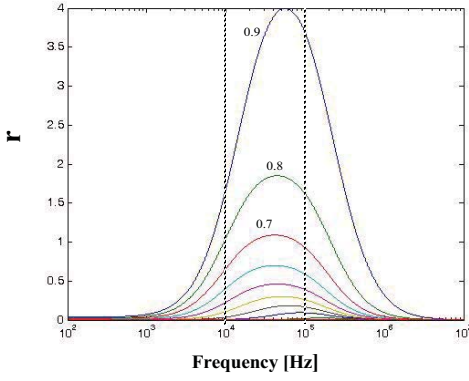


Fig. 5. Normalized magnitude impedance r for $ff=0.1$ to 0.9 in steps of 0.1

III. IMPEDANCE MEASURE CIRCUITS

New circuits required for sensing impedances have been implemented following the alternative feedback configuration in [13]. For the measure of impedance magnitude, Z_{xoc} , it will be considered that excitation signal is an AC current, with ω frequency. The circuits are designed to work maintaining a constant amplitude across the sensor ($V_{x0}=cte$), known as Pstat condition. The proposed circuit block diagram is shown in Fig. 6, and its main components are: the Instrumentation Amplifier (IA), the AC-to-DC converter or rectifier, the error amplifier, and the current oscillator with programmable output current. The voltage gain of the IA passband is α_{ia} . The rectifier works as a full wave peak-detector, to sense the biggest (lowest) voltage amplitude of V_o . Its output is a DC voltage, directly proportional to the amplitude of the instrumentation amplifier output voltage, with α_{dc} gain. The error amplifier, with α_{ea} gain, will compare the DC signal with a reference, V_{ref} , to amplify the difference. The voltage V_{ref} represents the constant voltage level required to works in Pstat mode. The current oscillator generates the AC current to excite the sensor. It is composed by an external AC voltage source, V_s , an OTA with g_m transconductance, and a four-quadrant voltage multiplier with K constant. The voltage generated by V_s , $V_{s0}\cdot\sin\omega t$, is multiplied by V_m , and then converted to a current by the OTA. The equivalent

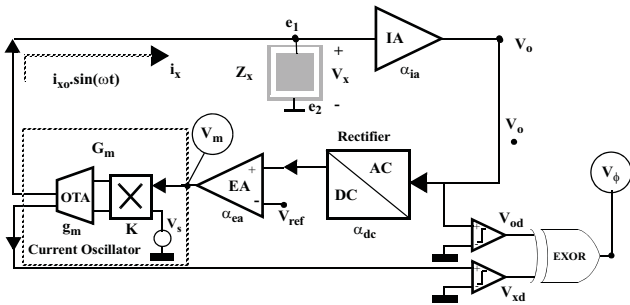


Fig. 6. Circuit blocks for impedance sensing.

transconductance from the magnitude voltage signal, V_m , to the excitation current, i_x , is called G_m and defined as $G_m = g_m \cdot V_{s0} \cdot K$. A simple analysis of the full system gives the approximated expression for the voltage amplitude at V_x ,

$$V_{x0} \approx \frac{V_{ref}}{\alpha_{ia} \alpha_{dc}} \quad (2)$$

when condition,

$$Z_{x0} G_m \alpha_{ea} \alpha_{ia} \alpha_{dc} \gg 1 \quad (3)$$

is satisfied. Voltage in eq. (2) remains constant if α_{ia} and α_{dc} are also constant. Hence, Pstat condition is fulfilled if condition given before is true. On other hand, considering the relationship between the current i_x and the voltage V_m ($i_{x0} = G_m \cdot V_m$), the magnitude of the impedance can be expressed as,

$$Z_{x0} = \frac{V_{x0}}{G_m} \cdot \frac{1}{V_m} \quad (4)$$

Equation (4) means that from voltage V_m , the impedance magnitude Z_{x0} can be calculated, since V_{x0} and G_m are known from eq. (2) and the design parameters. The impedance phase could also be measure with V_ϕ signal [13] in Fig. 6. The circuits have been designed in a $0.35\mu m$ CMOS technology for 3V power supply. Design parameters were adjusted for 10kHz frequency, with $Z_{x0} = 100k\Omega$. Parameters were chosen for $Z_{x0} G_m \alpha_{ia} \alpha_{dc} \alpha_{ea} = 100$. In particular, $\alpha_{ia} = 10$, $\alpha_{dc} = 0.25$, $\alpha_{ea} = 500$, $G_m = 1.2\mu S$, and $V_{ref} = 20mV$.

The instrumentation amplifier circuit schematic [15] is represented in fig. 7a. The passband frequency edges were designed according with the frequency sensitivity observed in fig. 5. The frequency response, magnitude and phase, is illustrated in fig. 7b for an input amplitude of 10mV. The full wave rectifier in fig. 8a is based on pass transistors (MP, MN) to load the capacitor C_r at the nearest voltage to $\alpha_{ia} V_o$ [16]. The two comparators detect if the input signal is higher (lower) than V_{op} (V_{om}) in order to charge the C_r capacitors. Discharge process of C_r is done by current sources, I_{dis} , and has been set to 1mV in a period. Figure 8b illustrates the waveforms obtained by electrical simulations for the upper and lower rectified signals at 10kHz. A two-stage open loop operational amplifier is used as error amplifier. For i_x amplitude programming, a four-quadrant multiplier [17] and an OTA were designed. The multiplier output waveforms ($V_m \times V_s$) are shown in fig. 9. In this figure, the AC signal V_s , has 200mV of amplitude at 10kHz frequency, is multiplied by a DC signal, V_m , in the range of $[0, 200mV]$. Finally, with data employed, V_x has an amplitude of 8mV. In electrode based measures, V_{x0} has typically low and limited values (tens of mV) to control the expected electrical performance of the electrodes [11].

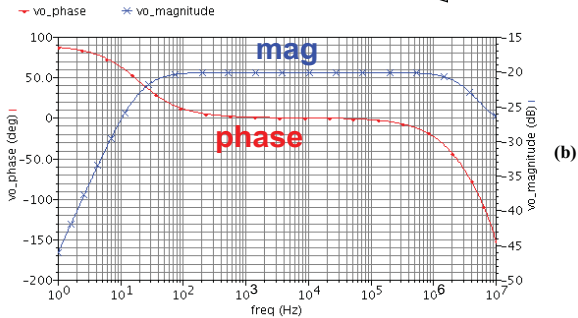
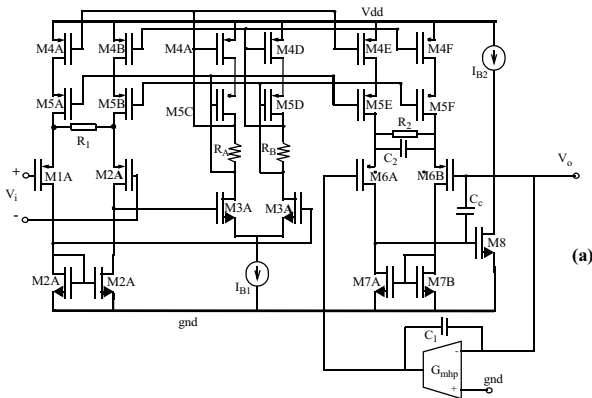


Fig.7. (a) CMOS Instrumentation Amplifier schematic. (b) Magnitude and phase frequency response for 10mV amplitude at the input.

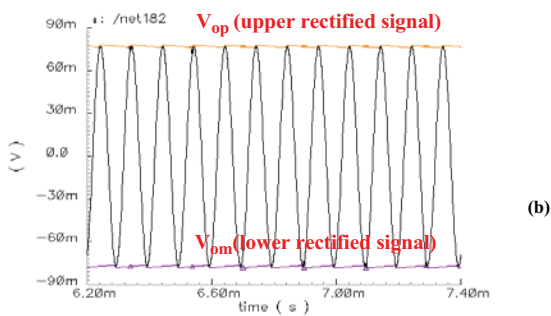
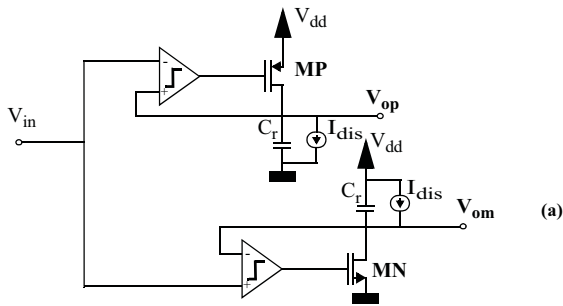


Fig.8. (a) Schematic for the full-wave rectifier. (b) Electrical simulations at 10kHz.

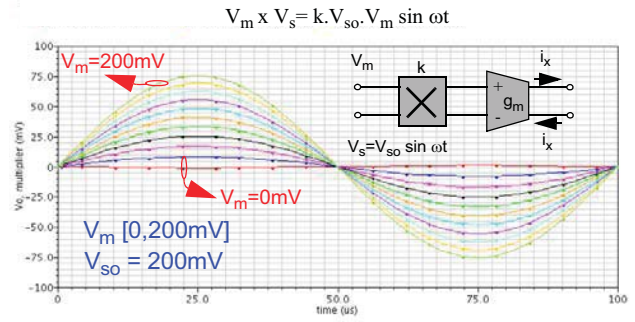


Fig.9. Simulated multiplier output voltage waveforms. The delivered AC current to electrodes (\$i_x\$) has an amplitude given by $i_x = (k \cdot g_m \cdot V_{so}) \cdot V_m$, in which can be considered $G_m = k \cdot g_m \cdot V_{so}$ as the equivalent transconductance from V_m input voltage to i_x output current. The amplitude of i_x can be programmed with the V_m voltage.

IV. SIMULATION RESULTS

To proof the proposed method for impedance sensing, we have chosen a simulation case with an 8x8 two-electrode array. The sample input to be analysed is a low density MCF-7 epithelial breast cancer cell culture shown in Fig. 10a. In this image, some areas are covered by cells and others are empty. Our objective is to employ the area parametrized electrode-cell model and the proposed circuits to detect their location. The selected pixel size is $50\mu m \times 50\mu m$, similar to cell dimensions. Figure 10a shows the grid and overlap with the image. We associate a squared impedance sensor to each pixel in Fig. 10a. To obtain a 2D system description valid for electrical simulation. Optimum pixel size can be obtained by using design curves for normalized impedance r and its frequency dependence. Each electrical circuit associated to each e_1 electrode in the array was initialized with its corresponding fill factor (ff). Matrix in Fig 10b is obtained in this way. Each electrode or pixel has associated a number in the range $[0,1]$ (ff) depending on its overlap with cells on top. These numbers were calculated with an

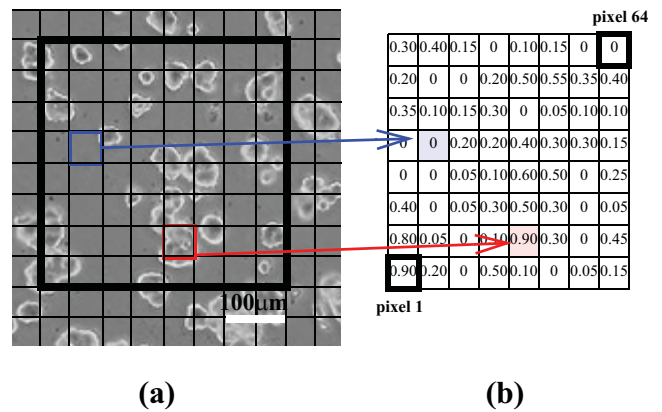


Fig.10. (a) 8x8 pixel area selection in epithelial breast cancer cell culture. (b) Fill factor map (ff) associated to each electrode (pixel).

accuracy of ± 0.05 from the image in Fig.10a. The ff matrix represents the input of our system to be simulated. Electrical simulations of the full system were performed at 10kHz (midband of the IA) to obtain the value of the voltage magnitude V_m in eq. (4) for all electrodes. Pixels are simulated by rows, starting from the left most down (pixel 1) to top most right (pixel 64). When measuring each pixel, V_m is reset to zero and then 25 cycles (N_c) are reserved to find its steady-state, where V_m value becomes constant and is acquired. In Fig. 12 are represented the waveforms obtained for the amplifier output voltage $\alpha_{ia}V_x$, voltage magnitude, V_m , and excitation current i_x . It is observed that the voltage at sensor, V_x , has always the same amplitude (8mV), while the current decreases with ff . The V_m signal converges towards a DC value, inversely proportional to the impedance magnitude. Steady-state values of V_m are represented in Fig. 11 for all pixels. These are used to calculate their normalized impedances r using eqs. (1) and (4).

pixel empty	65.3	61.0	66.6	67.8	67.7	67.7	67.8	67.8	
	67.2	67.6	67.7	55.0	55.0	51.5	63.5	61.0	
	63.5	67.8	67.5	65.2	67.8	67.8	67.7	67.7	
	67.8	67.8	67.2	67.2	61.0	65.2	65.2	67.7	
	67.8	67.8	67.6	67.7	48.1	55.0	67.8	66.4	
	61.0	67.8	67.5	65.1	55.1	65.3	67.7	67.7	
	32.8	67.8	67.8	67.6	25.0	65.3	67.8	58.2	
	25.0	67.2	67.8	55.0	67.7	67.8	67.7	67.6	pixel 90% full

Fig.11. Simulated V_m [mV] steady-state values at 10kHz frequency.

To have a graphical 2D image of the fill factor (covered area by cells) in all pixels, Fig. 13 represents the 8x8 ff -maps, in which each pixel has a grey level depending of its fill factor value (white is empty and black full). In particular, Fig. 13a represents the ff -map for the input image in Fig. 10a. Considering the parametrized curves in Fig. 5 at 10kHz frequency, fill factor parameter has been calculated for each electrode, using V_m simulated data from Fig. 11 and the results are represented in Fig. 13b. The same simulations have been

performed at 100kHz, achieving the ff -map in Fig. 13c. As Fig. 5 predicts, better matching with input is found at 100kHz because normalized impedance is more sensitive, having higher

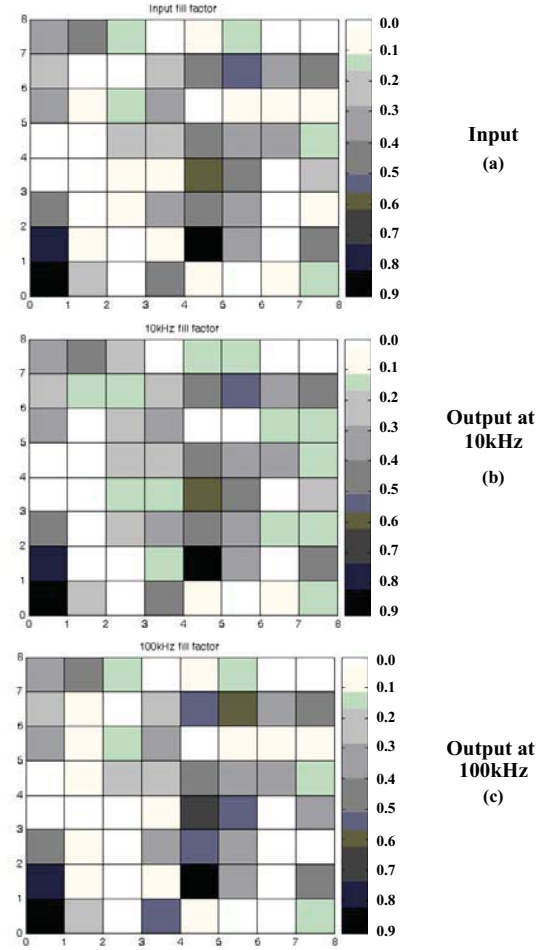


Fig.13. 2D diagram of the fill factor for 8x8 pixels: (a) ideal input, (b) image reconstructed from simulations at 10kHz and (c) from simulations at 100kHz.

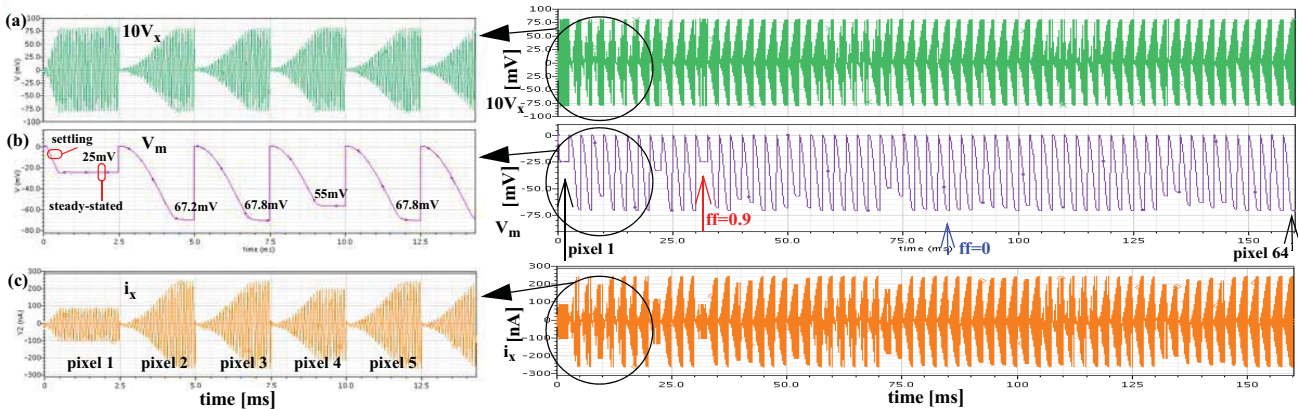


Fig.12. Simulated waveforms for (a) $\alpha_{ia}V_x = 10V_x$, (b) V_m and (c) i_x signals for the 64 electrodes at 10kHz.

dynamic range than at 10kHz. In both cases, errors obtained in \hat{f} values are below the 1%, so matching with input is excellent. The total time required to acquired data for a full image or frame will depend on measuring frequency, number of cycles reserve for each pixel ($N_c=25$ for reported example) and array dimension (8x8). For reported simulations, 160ms and 16ms for frame, working at 10kHz and 100kHz respectively, are required. This acquisition time by frame is enough for real time monitoring of cell culture systems.

V. CONCLUSIONS

This paper presents a novel system for impedance sensing of biological samples useful for 2D imaging. An electrical model based on the overlapping area is employed for electrode-cell characterization in both system simulation and image reconstruction. The proposed system works using Pstat approach and employs new circuit configuration for impedance measure in a feedback configuration, delivering easy to acquire signals and allowing to control the voltage amplitude on the electrodes. Electrical simulations have been done to reproduce ECIS technique, giving promising results in cell location and imaging, and enabling our system for other real time applications as cell index monitoring, cell tracking, etc. In future works, precise cell electrode model, optimized sensing circuits and design trade-off for electrode sizing will be further explored for a real experimental imaging system.

REFERENCES

- [1] J. J. Ackmann, "Complex Bioelectric Impedance Measurement System for the Frequency Range from 5Hz to 1MHz," *Annals of Biomedical Engineering*, vol 21, pp:135-146, 1993.
- [2] R. D. Beach, et al., "Towards a Miniature *In Vivo* Telemetry Monitoring System Dynamically Configurable as a Potentiostat or Galvanostat for Two- and Three- Electrode Biosensors," *IEEE Transactions on Instrumentation and Measurement*, vol 54, n°1, pp:61-72, 2005.
- [3] A. Yúfera et al., "A Tissue Impedance Measurement Chip for Myocardial Ischemia Detection". *IEEE transaction on Circuits and Systems: Part I*. vol.52, n°:12, pp:2620-2628. Dec. 2005.
- [4] S. M. Radke and E. C. Alocilja, "Design and Fabrication of a Microimpedance Biosensor for Bacterial Detection," *IEEE Sensor Journal*, vol 4, n° 4, pp: 434-440, Aug. 2004.
- [5] D. A. Borkholder: "Cell-Based Biosensors Using Microelectrodes," *PhD Thesis*, Stanford University. Nov. 1998.
- [6] I. Giaever et al., "Use of Electric Fields to Monitor the Dynamical Aspect of Cell Behaviour in Tissue Culture," *IEEE Transaction on Biomedical Engineering*, vol BME-33, n° 2, pp: 242-247, Feb. 1986.
- [7] D. Holder, "Electrical Impedance Tomography: Methods, History and Applications", *Philadelphia: IOP*, 2005.
- [8] A. Romani et al., "Capacitive Sensor Array for Location of Bioparticles in CMOS Lab-on-a-Chip," *International Solid Stated Circuits Conference (ISSCC)*, 12.4. 2004.
- [9] G. Medoro et al., "A Lab-on-a-Chip for Cell Detection and Manipulation," *IEEE Sensor Journal*, vol. 3, n° 3, pp: 317-325. Jun. 2003.
- [10] N. Manaresi et al., "A CMOS Chip for individual Cell Manipulation and Detection," *IEEE Journal of Solid Stated Circuits*, vol. 38, n° 12, pp: 2297-2305. Dec. 2003.
- [11] A. Hassibi et al.: "A Programmable 0.18 μ m CMOS Electrochemical Sensor Microarray for Biomolecular Detection," *IEEE Sensor Journal*, vol. 6, n° 6, pp:1380-1388. 2006.
- [12] X.Huang et al., "Simulation of Microelectrode Impedance Changes Due to Cell Growth," *IEEE Sensors Journal*, vol.4, n°5, pp: 576-583. 2004.
- [13] A. Yúfera et al., "A Method for Bioimpedance Measure With Four- and Two-Electrode Sensor Systems," *30th Annual International IEEE EMBS Conference*, pp: 2318-2321. Aug. 2008.
- [14] Neil Joye, et al., "An Electrical Model of the Cell-Electrode Interface for High-density Microelectrode Arrays," *30th Annual International IEEE EMBS Conference*, pp: 559-562. 2008
- [15] Y-Q. Zhao et al., "A CMOS Instrumentation Amplifier for Wideband Bioimpedance Spectroscopy Systems," *International Symposium on Circuits and Systems, ISCAS*, pp:5079-5082. 2006.
- [16] H. Ahmadi et al., "A Full CMOS Voltage Regulating Circuit for Bioimplantable Applications," *International Symposium on Circuits and Systems, ISCAS*, pp: 988-991, 2005.
- [17] C. Sawing et al., "Compact low-voltage CMOS four-quadrant analogue multiplier," *Electronics Letters*, vol.42, n° 20, pp: Sep. 2006